Improved Differential Attacks for ECHO and Grøstl

Thomas Peyrin

Ingenico, France
thomas.peyrin@ingenico.com

Abstract. We present improved cryptanalysis of two second-round SHA-3 candidates: the AES-based hash functions ECHO and Grøstl. We explain methods for building better differential trails for ECHO by increasing the granularity of the truncated differential paths previously considered. In the case of Grøstl, we describe a new technique, the internal differential attack, which shows that when using parallel computations designers should also consider the differential security between the parallel branches. Then, we exploit the recently introduced start-from-the-middle or Super-Sbox attacks, that proved to be very efficient when attacking AES-like permutations, to achieve a very efficient utilization of the available freedom degrees. Finally, we obtain the best known attacks so far for both ECHO and Grøstl. In particular, we are able to mount a distinguishing attack for the full Grøstl-256 compression function.

Key words: hash function, cryptanalysis, ECHO, Grøstl, AES, internal differential attack.

1 Introduction

Cryptographic hash functions are very important tools in cryptography, used in many applications such as digital signatures, authentication schemes or message integrity. Informally, a hash function H is a function that takes an arbitrarily long message as input and outputs a fixed-length hash value of size n bits. The classical security requirements for such a function are collision resistance and (second)-preimage resistance. Namely, it should be impossible for an adversary to find a collision (two distinct messages that lead to the same hash value) in less than $2^{n/2}$ hash computations, or a (second)-preimage (a message hashing to a given challenge) in less than 2^n hash computations. Moreover, those primitives are traditionally used to simulate the behavior of a random oracle [2] and while the community is divided on such a requirement, in the ideal case an attacker should not be able to distinguish a hash function from a random oracle.

As many standardized hash functions [39, 31] have been broken a few years ago [43, 42], the NIST launched in 2008 the SHA-3 competition [33] that will lead to the future hash function standard. 14 candidates among 51 have been selected for the second round and many of them (like ECHO [3], Grøstl [15] or SHAvite-3 [5]) are actually using some parts of the standardized block cipher AES [32, 10] as internal primitives or mimicking the structure of this cipher. While AES-256 can no more be considered as secure in the related-key model [7], major improvements [35, 20, 28, 26, 24, 27, 16] have recently been achieved regarding the cryptanalysis of AES-based hash functions. Those attacks make an extensive use of the freedom degrees that are available in a hash function and even provides the best known distinguishing attack against AES-128 [16] in the known-key model [22, 30]. However, the exhaustion of the available freedom degrees seems to indicate that a limit has currently been reached when attacking an AES-like permutation in a hash function. As we show in this paper, it is however possible to improve the differential techniques used so far.

Our contributions. In this paper, we improve the best known cryptanalysis results [1, 19, 28, 27, 16] on two second round SHA-3 candidates: the hash functions ECHO [3] and Grøstl [15]. While we do not provide advances regarding the freedom degrees optimization, we use the recently introduced Super-Sbox techniques [16, 14] in order to find pairs of inputs verifying a given differential path. We then exploit

some specific properties of ECHO and Grøstl to derive very good differential paths. More precisely, we improve the previously known truncated differential paths for ECHO by reducing the size of the truncated words considered. This allows us to broaden the differential trail search space, therefore increasing our probability to find a good path, but also augmenting the search complexity. We circumvent this constraint by giving a heuristic method to prune the potential candidates. Concerning Grøstl, we describe a novel yet simple cryptanalysis technique: the *internal differential attack*. It may be applied for functions using parallel branches that are not sufficiently made distinct. In that case, the attacker can find input instances (where a classical differential attack exhibits pairs of inputs) verifying non random properties on the output.

As a result, we are able to distinguish the full internal permutation of ECHO from a random 2048-bit permutation for a number of rounds corresponding to the full 256-bit version. While this attack does not convert into a distinguishing attack for the full compression function, we improve the best known results on reduced versions of ECHO for all hash output sizes in regards to both collision search and distinguishing attack. Moreover, we provide the first distinguishing attack on the full internal permutations for the 256-bit version of Grøstl, which can be directly derived into a distinguisher on the full Grøstl-256 compression function. Structural distinguishers (independent of the number of rounds) were already described in the original submission document [15]. For example, it was already identified that one can find fixed points or build a distinguisher for the compressions function with the generalized birthday paradox [41]. However, this structural distinguisher requires a very large amount of memory and offers a much smaller gap between its complexity and the generic attack than the ones presented in this paper. Our results are also interesting because they exploit the specificities of the internal permutations of Grøstl which is essential to really evaluate the security margin of this hash function in terms of number of rounds. All the results and the corresponding computation/memory complexities for ECHO and Grøstl are summarized in Table 1. The results concerning ECHO-SP (the simple-pipe version of ECHO) and the internal permutation of ECHO are given in Appendix. Note that none of the results described in this article seem to endanger the security of the whole ECHO or Grøstl hash functions.

Table 1. Summary of results for ECHO and Grøstl compression functions. ECHO-256 and ECHO-512 compression functions have 8 and 10 rounds respectively, while Grøstl-256 and Grøstl-512 compression functions have 10 and 14 rounds respectively.

target	rounds	computational complexity	memory requirements	type	section
ECHO-256 comp. function	3	2^{64}	2^{64}	semi-free-start collision[1]	this paper
	4	2^{64}	2^{64}	distinguisher	this paper
ECHO-512 comp. function	3	2^{96}	2^{64}	semi-free-start collision[1]	this paper
	6	2^{96}	2^{64}	distinguisher	this paper
Grøstl-256 comp. function	7	2^{56}		distinguisher	see [27]
	8	2^{112}	2^{64}	distinguisher	see [16]
	9	2^{80}	2^{64}	distinguisher	this paper
	10	2^{192}	2^{64}	distinguisher	this paper
Grøstl-512 comp. function	11	2^{640}	2^{64}	distinguisher	this paper

2 Previous cryptanalysis

In this section, we recall the recent advances regarding cryptanalysis of AES-like permutations and their specificities. In the rest of the paper, we will use the start-from-the-middle and Super-Sbox attacks as basic tool for finding input pairs verifying a given differential path.

[1] A semi-free-start collision can be found for the 4-round reduced ECHO-256 or ECHO-512 compression functions with complexity 2^{224} computations and 2^{64} memory, if the salt value can be controlled by the attacker.

2.1 Building differential trails with truncated differences

Cryptanalysis of AES-based hash functions began with the hash family proposal Grindahl [21] for which collision attacks have been found [35, 20]. This showed that truncated differentials [23] are very useful when cryptanalyzing a byte-oriented primitive such as the AES. Namely, instead of looking at the actual difference value of a byte, one only checks if a byte contains a difference (active byte) or not (inactive byte). In particular, this allows the attacker to handle the non-linear Sboxes quite nicely when building differential trails. On the other hand, the differential transitions through the linear MixColumns layer will now be verified probabilistically.

The matrix multiplication underlying the MixColumns transformation on a r-byte column for AES or Grøstl presents the interesting property of being a Maximum-Distance Separable (MDS) mapping: the number of active input and output bytes is always greater or equal to $r+1$ (unless there is no active input and output byte at all). When picking random inputs, the probability of success of a differential transition that meets the MDS constraints through a MixColumns layer is determined by the number of active bytes in the output. More precisely, if such a differential transition contains k active bytes in one column of the output, its probability of success will approximatively be equal to $2^{-8\times(r-k)}$. For example, a $4 \mapsto 1$ transition for one column of the AES MixColumns layer has success probability of approximatively 2^{-24}. Note that the same reasoning applies when dealing with the invert function of the MixColumns layer as well.

2.2 Rebound attacks

The rebound attack [28] is a new technique for using efficiently the available freedom degrees. The authors utilize truncated differential paths in which most of the cost lies in the middle rounds. Then, by using a local meet-in-the-middle-like technique, the freedom degrees are consumed in the middle part of the differential path, right where they can improve at best the overall complexity. More precisely, some rounds in the middle (the *controlled rounds*) will be verified with only a few operations on average, while the rest of the path both in forward and backward direction (the *uncontrolled rounds*) is fulfilled probabilistically. This cryptanalysis provides good results [26, 24] and can work without any special constraint on the differential path. However, the controlled part is limited to two rounds.

2.3 Start-from-the-middle attacks

In [27], the start-from-the-middle attack is introduced. It can be seen as a generalization of the previous technique: the idea is simply to use the freedom degrees in the "most expensive" part of the differential trail, without setting any constraint in the way this is handled. The "cheaper" parts are then covered in an inside-out manner in both forward and backward directions. The authors describe a freedom degrees use example that can control 3 rounds in the middle part, without increasing the complexity (i.e. with only a few operations). However, the depicted technique only works for specific differential paths, in which the number of active bytes in the controlled rounds is not too important. We refer to the original publication [27] for more details.

2.4 The Super-Sbox cryptanalysis technique

Finally, another example of start-from-the-middle attacks is the Super-Sbox cryptanalysis [16]. The idea is that one can view two rounds of an AES-like permutation as the parallel application of a layer of big Sboxes, named Super-Sboxes, preceded and followed by simple affine transformations. This technique can control 3-rounds in the middle of the differential trail with only a few operations on average, but works especially when the number of active bytes in the controlled rounds is important (this allowed to use longer differential paths which generally contain more active bytes). Because of some local precomputation steps, the drawback of this technique is its memory requirement when the size of the internal state of the scheme is too big. In the case of Grøstl this remains acceptable with a 2^{64} memory requirement, but in the case of ECHO as much as 2^{512} memory is required, making this tool unsuitable for this hash proposal. We refer to the original article [16] for more details.

3 Improved differential attack for ECHO

3.1 Description of ECHO

ECHO is a double-pipe hash function using HAIFA [4] as chaining iteration mode. The message to hash is first padded and divided into fixed-length blocks M_i which are used to update iteratively the chaining variable H_i (originally initialized with an initial vector $H_0 = IV$) thanks to the compression function h: $H_i = h(H_{i-1}, M_i)$. Finally, the hash output is obtained by truncating the last chaining variable. The compression function is built upon a 2048-bit AES-like permutation P_E^R composed of R rounds and its internal state can be viewed as a 4×4 matrix of 128-bit words (or cells). A cell will be denoted by $C_{i,j}$, where i is its row position and j its column position in the matrix, starting the counting from 0. One round of P_E^R is composed of three layers: the "BIG SubBytes" layer (big Sbox or B.SB), the "BIG ShiftRows" layer (B.ShR) and the "BIG MixColumns" layer (B.MC).

The BIG SubBytes layer is a non-linear function defined by the application of a big Sbox S on each 128-bit cell and this big Sbox is made of 2 AES rounds. The classical AddRoundKey part from the AES is not present in P_E^R and in order to avoid trivial symmetric vulnerabilities that would occur, each big Sbox in ECHO is distinct thanks to different subkey additions in each of the 2-round AES uses. The first round subkey depends on the value of a 64-bit internal counter K that is different at each use, while the second round subkey is set to the 128-bit salt value and thus always remains the same during the whole ECHO computation. So, for each cell $C_{i,j}$ of the internal state, we compute

$$C'_{i,j} = S[C_{i,j}] = AES_{salt}(AES_{0||K}(C_{i,j})).$$

where AES_{sk} denotes the application of one AES round with the subkey sk. As for the AES, the BIG ShiftRows transformation permutes the position of each cell in its own row: for each cell $C_{i,j}$ of the internal state, we compute $C'_{i,j} = C_{i,Sub_i(j)}$ where $Sub_i(j) = (j-i) \bmod 4$. Finally, the BIG MixColumns function is a linear function that mixes all the columns of the internal state separately. More precisely, the 32-bit AES MixColumns function is reused: if $C^b_{i,j}$ denotes the b-th byte of the cell $C_{i,j}$, then we compute

$$({C'}^b_{0,j}, {C'}^b_{1,j}, {C'}^b_{2,j}, {C'}^b_{3,j}) = AESMixColumns(C^b_{0,j}, C^b_{1,j}, C^b_{2,j}, C^b_{3,j})$$

for all $0 \leq j \leq 3$ and $1 \leq b \leq 16$. The round function on an internal state C can thus be defined as:

$$MixColumns \circ ShiftRows \circ SubBytes(C).$$

In the case of the ECHO-256 compression function, 8 rounds of the permutation are applied and a compressing phase is processed after the final feedforward. Namely, the compressing phase (denoted comp_{256}) xors all the four 512-bit columns together. Finally, the compression function takes a 1536-bit message input M (12 words) and a 512-bit chaining variable input H (4 words) and outputs a new 512-bit chaining variable H' with

$$H' = \mathsf{comp}_{256}(P_E^8(H||M) \oplus H||M)$$

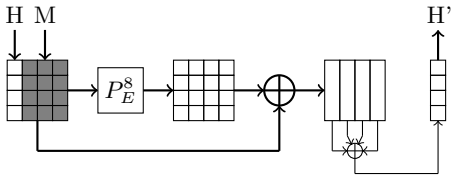

In the case of the ECHO-512 compression function, 10 rounds of the permutation are applied in order to turn a 1024-bit message input M (8 words) and a 1024-bit chaining variable input H (8 words) onto a new 1024-bit chaining variable H'. A different compressing phase is processed after the final feedforward.

$$H' = \mathsf{comp}_{512}(P_E^{10}(H||M) \oplus H||M)$$

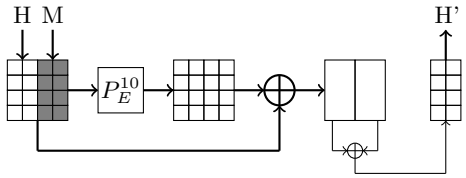

Namely, the compressing phase (denoted comp_{512}) xors the two first and the two last 512-bit columns together.
Since ECHO is a nested design of AES-like permutations, we will always use the prefix "BIG" when referring to one of the three layers of the 2048-bit permutation. When not using a prefix, we will refer to the layers of the 2-round AES permutation in the big Sboxes of ECHO.

In the following, $\mathsf{B.SB}_R^{in}$ (respectively $\mathsf{B.SB}_R^{out}$) will denote the whole internal state just before (respectively just after) application of the BIG SubBytes layer during round R (starting the counting from 0). Similarly, $\mathsf{B.MC}_R^{in}$ and $\mathsf{B.MC}_R^{out}$ will stand for the input and output internal states of the BIG MixColumns layer during round R. Of course, we have $\mathsf{B.SB}_R^{in} = \mathsf{B.MC}_{R-1}^{out}$. We refer to [3] for the full specifications.

3.2 Generic differential paths

In order to fully use the power of recent freedom degrees optimization techniques, the core of the differential path we use will not differ from the ones described in [28,27,16]. The reason here is that this core characteristic is perfectly fit for using the available freedom degrees in the middle: it is computationally very costly in its middle part, but quite cheap on its side parts. This core truncated differential path is 7 rounds long and is depicted in Figure 1. Of course, when attacking a smaller number of rounds than 7, one can use this core to build a further reduced path by cutting off some of the first and/or last rounds.

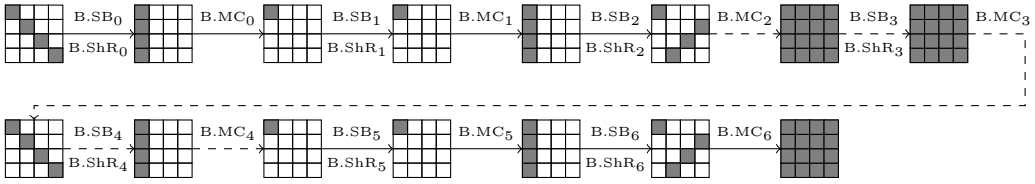

Fig. 1. Core of the truncated differential paths for 7-round reduced ECHO internal permutation. Each cell represents a 128-bit word and a gray cell stands for an active 128-bit word. The controlled rounds are depicted with dashed lines.

The second advantage of this core characteristic is that the relatively low number of active cells in the controlled rounds makes it usable with the start-from-the-middle technique, as it is described in [27]: one can find a pair of internal states verifying the 128-bit truncated differential trail from the beginning of round 2 ($\mathsf{B.SB}_2^{in}$) up to the end of round 4 ($\mathsf{B.MC}_4^{out}$) with only one operation on average (and 2^{64} memory). Note that another view of the attack is to say that with one operation the attacker can find a pair of internal states such that the difference on $\mathsf{B.SB}_2^{out}$ and on $\mathsf{B.MC}_4^{out}$ are chosen (no more truncated differentials). Therefore, for ECHO we consider that the controlled rounds go from $\mathsf{B.SB}_2^{out}$ up to $\mathsf{B.MC}_4^{out}$.

One can easily check that the rest of the path (the uncontrolled rounds) is fulfilled with probability one, except round 1. Indeed, in round 1, a $4 \Rightarrow 1$ truncated differential transition is expected through

the backward computation of the BIG MixColumns layer $\mathsf{B.MC}_1$. When dealing with 128-bit truncated differentials, this will happen with approximate probability $2^{-24\times16} = 2^{-384}$ (i.e. a $4 \Rightarrow 1$ byte-wise truncated differential transition is expected through sixteen parallel $AESMixColumns$ functions) and this probability sets the overall 2^{384} complexity for finding a valid pair for the core path from Figure 1. We will see in the next section that by looking at byte-wise truncated differentials (instead of word-wise), one can sharpen the differential path and improve the success probability of this BIG MixColumns layer. On the other side, in order to be able to use the byte-wise truncated differentials at this stage and since she can control the difference only in $\mathsf{B.SB}_2^{out}$ (and not in $\mathsf{B.SB}_2^{in}$), the attacker will have to handle the backward computation of the BIG SubBytes layer of round 2 ($\mathsf{B.SB}_2$) as well. She then hopes that controlling both $\mathsf{B.SB}_2$ and $\mathsf{B.MC}_1$ with byte-wise truncated differentials will cost less than 2^{384} operations. Not controlling $\mathsf{B.SB}_2$ would lead us back to the 128-bit truncated differential cryptanalysis, as each active 128-bit word of $\mathsf{B.SB}_2^{in}$ will very likely contain 16 active bytes (i.e. fully active word) since full diffusion is achieved with two `AES` rounds.

3.3 Differential transitions for 2 `AES` rounds

Now that we introduced the core of the differential path, we need to study the word-wise differential transitions. That is, instead of looking for 128-bit truncated differentials, we will look at byte-wise truncated differentials. Of course, we still fully leverage the previous works on start-from-the-middle attacks [27]: the attacker can find a valid candidate pair verifying the controlled rounds and fully control the differences in $\mathsf{B.SB}_2^{out}$ and $\mathsf{B.MC}_4^{out}$ with one operation on average. Sharpening the differential path will improve the results since our scope is now wider, but it will also greatly increase the number of potential trails and complicate the analysis. For that reason, we need to heuristically filter them so that we place our search into a good subspace. First, we restrict ourselves to four types of byte-wise truncated differential words `F`, `C`, `D` and `1`, all depicted in Figure 2. Due to symmetry and diffusion considerations, we believe that analyzing other differentials would not provide better results, while it would greatly increase the search space. Secondly, we add the constraint that all the active 128-bit words in an internal state will present the same byte-wise truncated differential (all words have the same truncated differential types `F`, `C`, `D` or `1`). This seems a sound constraint as the processing of the BIG MixColumns layer on one word column of the internal state can be seen as the parallel application of sixteen $AESMixColumns$ functions (one for each byte position). Thus, for each word column, instead of analyzing the behavior of sixteen parallel $AESMixColumns$ functions one conceptually only handles a single function that will do for all the 16. Those two filters will really simplify the analysis.

Fig. 2. Byte-wise truncated differential states for one word of `ECHO`. Each cell represents a byte and a gray cell stands for an active byte.

Since the attacker will have to control the behavior of BIG SubBytes layer $\mathsf{B.SB}_2$, we have to study the success probability for each possible transition for 2 `AES` rounds between the four bit-wise truncated differentials `F`, `C`, `D` and `1`, especially in backward direction. First, we can compute the approximate probability of success for a one round transition between those four 128-bit differential states and this is given in Table 2 for both forward and backward directions. Those probabilities are simply obtained by studying the $AESMixColumns$ transitions in one `AES` round (since we are dealing with byte-wise truncated differentials, all the probabilities comes only from the $AESMixColumns$ transitions, see [35]).

Table 2. Byte-wise truncated differential transition approximated probabilities for one round of AES. The left table shows forward transitions, while the right one gives backward transitions.

Forward				
in \ out	F	C	D	1
F	1	0	2^{-96}	0
C	1	0	0	0
D	0	1	0	2^{-24}
1	0	1	0	0

Backward				
in \ out	F	C	D	1
F	1	2^{-96}	0	0
C	0	0	1	2^{-24}
D	1	0	0	0
1	0	0	1	0

When computing backward through $\mathsf{B.SB}_2$, the *AESMixColumns* function from the second AES round is the first function to invert. But since this layer is fully linear, one can verify the expected backward transitions by carefully choosing the differences in $\mathsf{B.SB}_2^{out}$ beforehand. Since the start-from-the-middle attack allows us such a liberty, the second AES round in $\mathsf{B.SB}_2$ comes for free (one only has to check that the transition is not impossible, i.e. the probability in Table 2 is not null). Finally, having set all the constraints and the cost evaluation, we only have to pick the best backward differential transition through $\mathsf{B.SB}_2$ in terms of probability and active byte weight: $\mathtt{D} \Leftarrow \mathtt{1} \Leftarrow \mathtt{C}$. The transition $\mathtt{D} \Leftarrow \mathtt{1}$ is free as showed by Table 2, while the 2^{-24} probability for the transition $\mathtt{1} \Leftarrow \mathtt{C}$ is not taken in account since we can avoid it by carefully choosing the byte-wise truncated differences in $\mathsf{B.SB}_2^{out}$ beforehand. Therefore, controlling $\mathsf{B.SB}_2$ is now completely free for the attacker.

Now that we controlled the differential behavior of $\mathsf{B.SB}_2$, what is the improvement obtained for the BIG MixColumns layer $\mathsf{B.MC}_1$? Since we only have four active bytes in D, we can focus on controlling 4 parallel *AESMixColumns* transitions instead of 16. We are looking for $4 \Rightarrow 1$ transitions, each happening with probability 2^{-24}. Thus, for the whole BIG MixColumns layer, we get a probability of $2^{-24\times 4} = 2^{-96}$ and this has to be compared to the previous $2^{-24\times 16} = 2^{-384}$ probability.

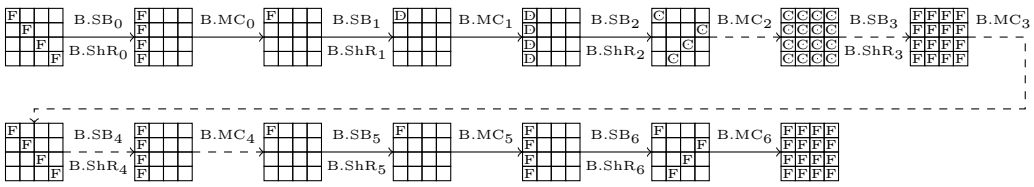

Fig. 3. 7-round differential path for the ECHO internal permutation. The controlled rounds are depicted with dashed lines.

Overall the whole 7-round differential path is depicted in Figure 3 and a valid candidate can be found with complexity 2^{96} operations and 2^{64} memory. Since the internal permutation of ECHO is much bigger than its hash output size, it should be easy to distinguish it from a random 2048-bit permutation. Note that our solution pair has four active 128-bit words in the input and four active 128-bit words in the output (the last BIG MixColumns call is not taken in account since it is fully linear). A naive analysis would conclude that for a random 2048-bit permutation, finding such a pair with a birthday paradox technique should require at least $2^{(2048-512)/2} = 2^{768}$ operations. However, since the input and output amount of differences is low, the attacker can not fully leverage the power of the birthday paradox. We conclude by reusing the concept of *limited birthday distinguishers* [16] that for a random

2048-bit permutation, finding such a pair should require at least 2^{1024} operations[1]. Finally, 7 rounds of the internal permutation of ECHO can be distinguished from a random 2048-bit permutation with 2^{96} operations and 2^{64} memory.

The amount of freedom degrees available during the attack is discussed in the Appendix A and a costly distinguisher for 8 rounds of the ECHO internal permutation is given in Appendix B.

4 Internal differential attack: application to Grøstl

4.1 Description of Grøstl

We give in this section the description of Grøstl and refer to the submission document [15] for more details. Grøstl is a double-pipe hash function that uses a chaining mode similar to the Merkle-Damgård [29, 11] iteration. More precisely, after having initialized the internal state H_0 and padded the input message string, the iteration i updates the $2n$-bit chaining variable H_i with the $2n$-bit incoming message block M_i by applying the compression function h: $H_i = h(H_{i-1}, M_i)$. After having processed all the t message blocks, an output function is applied to the last chaining variable to obtain the n-bit hash result: $hash = trunc_n(P(H_t) \oplus H_t)$, where $trunc_n$ is the truncation function of the n first bits and P is an AES-based permutation. The double-pipe compression function h is built upon two similar parallel AES-based permutations P and Q (that only differ by the constants addition layers) to update chaining variable H with message block M:

$$H' = P(H \oplus M) \oplus Q(M) \oplus H$$

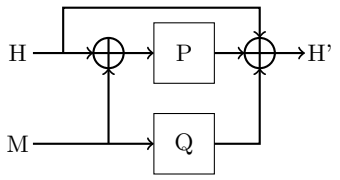

In the case of Grøstl-256, the 512-bit internal state of both permutations can be viewed as a 8×8 matrix of bytes. A byte for permutation P is denoted by $CP_{i,j}$ (resp. $CQ_{i,j}$ for permutation Q), where i is its row position and j its column position in the matrix, starting the counting from 0. P and Q are both 10-round long and each round is composed of 4 layers. The first layer (AddConstant or AC) is a constant addition function. More precisely, for the round number i (starting the counting from 0), in P the byte $CP_{0,0}$ is xored with i and in Q the byte $CQ_{7,0}$ is xored with $i \oplus$ 0xff. **Note that this layer is the only difference between permutations P and Q.** The second layer (SubBytes or SB) is a non-linear function defined by the application of the AES Sbox S to each byte. The third layer (ShiftRows or ShR) cyclically rotates to the left the position of each byte in its own row with the following constants: $(0, 1, 2, 3, 4, 5, 6, 7)$. Finally, the last layer (MixColumns or MC) is a linear function that mixes all the columns of the internal state separately. As for $AESMixColumns$, the matrix multiplication underlying this transformation is a Maximum-Distance Separable mapping. In order to avoid overweighting the notations, we used the same notations for the ECHO and Grøstl subfunctions, but their meaning is implicit depending on which scheme we are dealing with. The round function on an internal state C can thus be defined as:

$$MixColumns \circ ShiftRows \circ SubBytes \circ AddConstant(C).$$

In the case of Grøstl-512, the 1024-bit internal state of both permutations can be viewed as a 8×16 matrix of bytes. P and Q are both 14-round long and each round is composed of the 4 layers. The

[1] The generic attack complexity for mapping through a permutation a fixed difference on i bits on the input and j bits on the output with $i \geq j$ is given by the formula $\max\{2^{j/2}, 2^{i+j-t}\}$, where t is the size of the permutation.

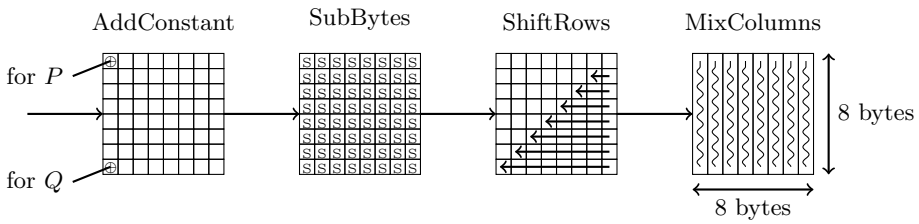

round function is identical to the Grøstl-256 case, except the rotation constants in the third layer: $(0, 1, 2, 3, 4, 5, 6, 11)$.

4.2 The internal differential attack

In this section, we will show that very good differential trails can be found for Grøstl. Our new technique, ***the internal differential attack***, may apply when a function is built upon parallel computation branches that are not distinct enough. The trick is **to devise a differential path representing the differences between the branches and not between two inputs of the function**. Usually this is avoided by a forcing strong separation between the two parallel branches. For example, for all steps of the hash function RIPEMD [37, 12], very distinct constants are used in the left and right branches. However, in the case of Grøstl, this separation is thin between permutations P and Q, and we will describe in the next sections how to exploit this property in order to mount for example a distinguishing attack against the full Grøstl-256 compression function.

All the previous analysis of Grøstl studied the differential behavior of the permutations in a classic way. That is, they derived differential trails by dealing with two different inputs for each of the permutations P and Q (the two permutations were attacked separately). Those permutations mimicking the AES block cipher, the best usable differential paths naturally reached 8 rounds [16], but we argue that much more interesting trails can be built. We do not analyze the two permutations separately, but we build a differential path **between them**: we keep track of the differences ongoing between branch P and branch Q (see Figure 4). We compute two internal states A and B, such that $A \oplus B = \Delta_{IN}$ and such that $P(A) \oplus Q(B) = \Delta_{OUT}$.

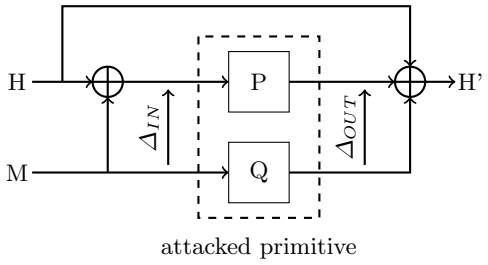

Fig. 4. The differential paths keep track of the differences between permutations P and Q.

This idea comes naturally after having noticed that permutations P and Q are really similar, since their only distinction is the constant addition phase. Even in that step, the distinction is really thin: a different constant is added on only two different bytes. Thus, we can hope that the amount of differences will remain low when setting a differential trail.

Since using truncated differentials is very handy when attacking AES-like permutations, we will only keep track of active and inactive bytes through the path. Also, preparing for the utilization of Super-

Sbox attacks, we aim for a differential path in which the costly part lies in the middle, and the cheap parts on the sides. In Figure 14 and 15 from the Appendix E, we provide a differential path between the permutations P and Q of the Grøstl-256 compression function for the 9-round and the 10-round versions respectively. In Figure 16 from the Appendix E, we depict a differential path between the permutations P and Q of the Grøstl-512 compression function reduced to 11 rounds. Note that only one difference is incorporated during AC_0 since the constant added in P is 0.

4.3 Deriving a distinguisher for Grøstl

In the following, our goal is to distinguish the Grøstl compression function from an ideal primitive on the same domain. As shown in Figure 4, once the differential path settled, we find a valid pair of internal states (A, B) such that

$$A \oplus B = \Delta_{IN}$$
$$P(A) \oplus Q(B) = \Delta_{OUT}$$

where Δ_{IN} and Δ_{OUT} are respectively the input and output truncated differences. We then set $H = A \oplus B$ and $M = B$ and we obtain

$$h(H, M) = P(A) \oplus Q(B) \oplus A \oplus B = \Delta_{IN} \oplus \Delta_{OUT}.$$

We will show that Δ_{IN} and Δ_{OUT} are always maintained in a small subspace. As a consequence, $\Delta_{IN} \oplus \Delta_{OUT}$ will also belong to a small subspace of the full output domain. Said in other words, we will be able to compute outputs of the $2n$-bit compression function that always belong to a predetermined set of k elements. In the ideal case, one such output should not be obtained with substantially less than $2^{2n}/k$ compression function calls. Unlike the previously known distinguishers that find partially colliding outputs for AES-like permutations, the one we describe here is more "preimage" oriented.

While formally defining a distinguisher for a keyless primitive is difficult [38], we argue that the property we exhibit here works for any choice of Sbox, MixColumns function or AddConstant positions for example. This clearly indicates that one could define a parametrized family of Grøstl-like compression functions, such that an attacker can exhibit an output maintained in the set of k elements for any member of the family. Moreover, note that such keyless primitive distinguishers have already been utilized in [27, 16].

5 Results

In this section we present our results on the compression functions of ECHO and Grøstl. For completeness, we give in the Appendix D the analysis for the single-pipe version ECHO-SP. Moreover, we also provide in the Appendix A a study of the amount of freedom degrees available during the attacks.

5.1 ECHO

Compression function distinguishers. We provide here the first distinguishers for reduced ECHO compression functions. In the case of ECHO-256, we use the 4-round differential path from Figure 8 in the Appendix C which is derived from the 7-round core path. One can find a solution with 2^{64} computations and memory (2^{39} valid candidates can be generated by the attacker and 2^{167} if the salt is controlled as well). In the case of ECHO-512, we use the 6-round differential path from Figure 9 in the Appendix C for which a solution can be found with 2^{96} computation and 2^{64} memory (2^{71} valid candidates can be generated by the attacker and 2^{199} if the salt is controlled as well). In both cases, we obtain compression function outputs colliding on 2 predetermined words (i.e. 256 bits) and this should require 2^{128} computations in the ideal case.

Collision attacks. We provide here the first collision attacks for reduced ECHO compression functions. In the case of ECHO-256, we use a special 3-round differential path depicted in Figure 10 from the Appendix C. In this trail, the start-from-the-middle technique can still be used and the only part uncontrolled is the first AES round of the very first BIG SubBytes layer. However, since we use the backward transition D $\Leftarrow$ 1 $\Leftarrow$ C, this layer will behave as expected with probability 1. Then, the feedforward is applied and only four 128-bit words will be active, each containing 4 active bytes at the exact same positions (truncated differential of type D). Finally, since the four columns of 128-bit words are xored together to obtain the output chaining variable, a collision can occur if the truncated differences are erased on the 4 byte positions. Thus, in order to get a semi-free-start collision, one should therefore test 2^{32} candidates (we have enough freedom degrees since one can generate 2^{143} valid candidates for the whole trail and 2^{271} if the salt is chosen by the attacker). However, the minimum cost for using the start-from-the-middle attack for ECHO is 2^{64} memory and precomputation. Thus, the overall cost is 2^{64} computations and memory in order to find one single semi-free-start collision for 3 rounds.

In the case of ECHO-512, we use the 4-round differential path from Figure 11 in the Appendix C for which a solution can be found with 2^{96} computations and 2^{64} memory (2^{71} valid candidates can be generated by the attacker and 2^{199} if the salt is controlled as well). Then, the feedforward is applied and one active 128-bit word remains in the output. In order to erase this difference and obtain a semi-free-start collision, this should be repeated 2^{128} times and the total cost of the attack is then 2^{224} computations and 2^{64} memory. Thus, this attack is valid only in the chosen-salt attacker model (otherwise the number of available freedom degrees is not sufficient). Since the collision happens before the final compression phase, this semi-free-start collision attack applies with the same complexity to ECHO-256 compression function.

When the attacker can not control the salt value, the 3-round attack from Figure 12 in the Appendix C applies. Namely the reasoning is exactly the same as for the 256-bit case with Figure 10, except that we have 4 additional bytes to collide during the feedforward phase. Finally, finding a semi-free-start collision for the 3-round reduced ECHO-512 compression function requires 2^{96} computations and 2^{64} memory.

5.2 Grøstl

Grøstl-256. We use the Super-Sbox technique to find two 512-bit internal states such that the 9-round differential path from Figure 14 between permutations P and Q is verified. Namely, one can find internal state values for P and Q verifying the truncated differential trail from the output of SB_2 up to the input of SB_5 with one computation on average. However, the $8 \mapsto 2$ MixColumns transition through MC_5 during the uncontrolled rounds is verified with probability 2^{-48}. Also, 2 byte differences must be erased during both AddConstant functions AC_2 and AC_6 which adds another $2^{-4\times 8} = 2^{-32}$ factor. Overall, one can find a valid candidate for the whole path with only $2^{48+32} = 2^{80}$ computations (an amount of 2^{64} memory is required by the Super-Sbox technique).

Regarding the 10-round differential path from Figure 15, the controlled rounds go from the output of SB_3 up to the input of SB_6. Then, the two $8 \mapsto 1$ MixColumns transitions through MC_2 and the $8 \mapsto 2$ transition through MC_6 during the uncontrolled rounds happen with probability $2^{-2\times 56} = 2^{-112}$ and 2^{-48} respectively. Also, 2 byte differences must be erased during both AddConstant functions AC_2 and AC_7 which adds another $2^{-4\times 8} = 2^{-32}$ factor. Overall, one can find a valid candidate for the whole path with only $2^{112+48+32} = 2^{192}$ computations (again, an amount of 2^{64} memory is required by the utilization of the Super-Sbox technique).

The freedom degrees analysis from Appendix A shows that for both paths from Figure 14 and 15, one can expect to obtain one solution.

Grøstl-512. As for Grøstl-256, we use the Super-Sbox technique to find two 1024-bit internal states such that the 11-round differential path from Figure 16 between permutations P and Q is verified. Namely, one can find internal state values for P and Q from the output of SB_3 up to the input of SB_6 with

one computation on average. However, the MixColumns transition through MC_6 during the uncontrolled rounds happens with probability $2^{-(48+7\times 56)} = 2^{-440}$: the first column is a $8 \mapsto 2$ transition, while the second, third, fourth, fifth, sixth, seventh and twelfth are $8 \mapsto 1$ transitions. The next MixColumns layer MC_7 contains a $8 \mapsto 2$ transition, adding another factor 2^{-48}. Regarding MC_2, the first and sixth columns are $8 \mapsto 1$ transitions, thus successfully verified with a total probability of $2^{-2\times 56} = 2^{-112}$. Also, 2, 1 and 2 byte differences must be erased during AddConstant functions AC_2, AC_7 and AC_8 respectively. This adds another $2^{-5\times 8} = 2^{-40}$ factor. Overall, one can find a valid candidate for the whole path with $2^{440+48+112+40} = 2^{640}$ computations (an amount of 2^{64} memory is required by the Super-Sbox technique for `Grøstl`). Again, the freedom degrees analysis shows that we can expect one solution.

The distinguisher for `Grøstl`. In order to mount the distinguisher for `Grøstl`, one has to analyze the amount k of reachable output difference values. The situation is completely identical for the paths from Figures 14 and 15 in the Appendix, but we will use the notations from the second one. We have 16 active bytes just before applying the very last MixColumns layer MC_9. Since the MixColumns layer is fully linear, the amounts of reachable difference values on its input and on its output are equal. Thus, we can deduce that at most $2^{16\times 8} = 2^{128}$ distinct output differences can be reached on the output of the differential trail. Regarding the input of the path, the same reasoning gives us that at most $2^{8\times 8} = 2^{64}$ distinct input differences can be reached. Note that the difference inserted during AC_0 can be ignored since it is the last layer when computing backward (the difference value on that byte will always be equal to the constant added). Also, it is easy to verify that the differences on the output of SB_0 are always the same (since MixColumns is linear). Thus, since the inverse of the `AES` Sbox has the property that only 2^7 distinct output differences can be reached when the input difference is fixed, we can conclude that Δ_{IN} can go through a maximum of $2^{8\times 7} = 2^{56}$ distinct values.

To summarize, the output chaining variable $H' = h(H, M) = \Delta_{IN} \oplus \Delta_{OUT}$ is limited to a set of at most $k = 2^{128+56} = 2^{184}$ values. For an ideal 512-bit compression function, reaching any element of this set should require $2^{512-184} = 2^{328}$ operations. With 2^{80} and 2^{192} computations respectively (and 2^{64} memory), we finally conclude that our attack can distinguish 9-round reduced or the full 10-round compression function of `Grøstl`-256 from a random 512-bit compression function.

In the case of `Grøstl`-512 (see Figure 16 in the Appendix E), the same reasoning tells us that Δ_{IN} can go through a maximum of 2^{56} values and Δ_{OUT} through a maximum of 2^{128} values. Thus, the output chaining variable $H' = h(H, M) = \Delta_{IN} \oplus \Delta_{OUT}$ is limited to a set of at most $k = 2^{128+56} = 2^{184}$ values. For an ideal 1024-bit compression function, reaching any element of this set should require $2^{1024-184} = 2^{840}$ operations. We conclude that our 2^{640} computations (and 2^{64} memory) attack can distinguish a 11-round reduced version of the `Grøstl`-512 compression function from a random 1024-bit compression function.

Note that structural distinguishers (i.e. working for randomly chosen permutations P and Q) already exist for `Grøstl`. For example, just like in the Davies-Meyer construction, one can very easily find fixed points for the compression function. Yet, we believe that our distinguishers are very interesting because they exploit the real differential properties of the internal permutations P and Q, which is essential in order to appropriately evaluate the security margin in terms of number of rounds.

6 Conclusion

In this article, based on recent advances on `AES`-like permutations studies, we provided a new cryptanalysis of `ECHO` and `Grøstl`, two second-round `SHA-3` candidates. In particular, in the case of `Grøstl`, we introduce a new cryptanalysis technique: the internal differential attack. Overall, we obtain the best cryptanalysis results known so far for both `ECHO` and `Grøstl`. We are able to derive a distinguisher for the full (10 rounds) 256-bit version of the `Grøstl` compression function. This work also shows that designers must be careful when building a function with parallel branches computations as the internal differential paths may lead to unexpected attacks.

Acknowledgments

The author would like to thank the `Grøstl` team and Henri Gilbert for their helpful comments.

References

1. P.S.L.M. Barreto. An observation on Grøstl. Comment submitted to the NIST hash function mailing list, hash-forum@nist.gov. `http://www.larc.usp.br/~pbarreto/Grizzly.pdf`.
2. Mihir Bellare and Phillip Rogaway. Random oracles are practical: A paradigm for designing efficient protocols. In *ACM Conference on Computer and Communications Security*, pages 62–73, 1993.
3. Ryad Benadjila, Olivier Billet, Henri Gilbert, Gilles Macario-Rat, Thomas Peyrin, Matt Robshaw, and Yannick Seurin. SHA-3 Proposal: ECHO. Submission to NIST, 2008. Available online at `http://crypto.rd.francetelecom.com/echo/`.
4. Eli Biham and Orr Dunkelman. A framework for iterative hash functions: Haifa. Second NIST Cryptographic Hash Workshop, 2006.
5. Eli Biham and Orr Dunkelman. The shavite-3 hash function. Submission to NIST, 2008.
6. Alex Biryukov, editor. *Fast Software Encryption, 14th International Workshop, FSE 2007, Luxembourg, Luxembourg, March 26-28, 2007, Revised Selected Papers*, volume 4593 of *Lecture Notes in Computer Science*. Springer, 2007.
7. Alex Biryukov, Dmitry Khovratovich, and Ivica Nikolic. Distinguisher and Related-Key Attack on the Full AES-256. In Halevi [17], pages 231–249.
8. Gilles Brassard, editor. *Advances in Cryptology - CRYPTO '89, 9th Annual International Cryptology Conference, Santa Barbara, California, USA, August 20-24, 1989, Proceedings*, volume 435 of *Lecture Notes in Computer Science*. Springer, 1990.
9. Ronald Cramer, editor. *Advances in Cryptology - EUROCRYPT 2005, 24th Annual International Conference on the Theory and Applications of Cryptographic Techniques, Aarhus, Denmark, May 22-26, 2005, Proceedings*, volume 3494 of *Lecture Notes in Computer Science*. Springer, 2005.
10. Joan Daemen and Vincent Rijmen. *The Design of Rijndael*. Information Security and Cryptography. Springer, 2002. ISBN 3-540-42580-2.
11. Ivan Damgård. A Design Principle for Hash Functions. In Brassard [8], pages 416–427.
12. H. Dobbertin, A. Bosselaers, and B. Preneel. RIPEMD-160: A Strengthened Version of RIPEMD. In D. Gollmann, editor, Fast Software Encryption – FSE 96, volume 1039 of *Lecture Notes in Computer Science*, pages 71–82. Springer, 1996.
13. Orr Dunkelman, editor. *Fast Software Encryption, 16th International Workshop, FSE 2009, Leuven, Belgium, February 22-25, 2009, Revised Selected Papers*, volume 5665 of *Lecture Notes in Computer Science*. Springer, 2009.
14. Florian Mendel and Christian Rechberger and Martin Schläffer and Søren Steffen Thomsen. Rebound Attacks on the Reduced Grøstl Hash Function. In Josef Pieprzyk, editor, *Topics in Cryptology - CT-RSA 2010*, LNCS. Springer, 2010. to appear.
15. Praveen Gauravaram, Lars R. Knudsen, Krystian Matusiewicz, Florian Mendel, Christian Rechberger, Martin Schläffer, and Søren S. Thomsen. Grøstl – a SHA-3 candidate. Submission to NIST, 2008. Available online at `http://www.groestl.info`.
16. Henri Gilbert and Thomas Peyrin. Super-Sbox Cryptanalysis: Improved Attacks for AES-like Permutations. In Fast Software Encryption – FSE 2010, volume to appear of *Lecture Notes in Computer Science*. Springer, 2010. Available online at `http://eprint.iacr.org/2009/531`.
17. Shai Halevi, editor. *Advances in Cryptology - CRYPTO 2009, 29th Annual International Cryptology Conference, Santa Barbara, CA, USA, August 16-20, 2009. Proceedings*, volume 5677 of *Lecture Notes in Computer Science*. Springer, 2009.
18. Michael J. Jacobson Jr., Vincent Rijmen, and Reihaneh Safavi-Naini, editors. *Selected Areas in Cryptography, 16th Annual International Workshop, SAC 2009, Calgary, Alberta, Canada, August 13-14, 2009, Revised Selected Papers*, volume 5867 of *Lecture Notes in Computer Science*. Springer, 2009.
19. J. Kelsey. Some notes on Grøstl. Comment submitted to the NIST hash function mailing list, hash-forum@nist.gov. `http://ehash.iaik.tugraz.at/uploads/d/d0/Grostl-comment-april28.pdf`.
20. Dmitry Khovratovich. Cryptanalysis of Hash Functions with Structures. In Jr. et al. [18], pages 108–125.
21. Lars R. Knudsen, Christian Rechberger, and Søren S. Thomsen. The Grindahl Hash Functions. In Biryukov [6], pages 39–57.

22. Lars R. Knudsen and Vincent Rijmen. Known-Key Distinguishers for Some Block Ciphers. In K. Kurosawa, editor, *ASIACRYPT*, volume 4833 of *Lecture Notes in Computer Science*, pages 315–324. Springer, 2007.
23. L.R. Knudsen. Truncated and Higher Order Differentials. In B. Preneel, editor, Fast Software Encryption – FSE 1994, volume 1008 of *Lecture Notes in Computer Science*, pages 196–211. Springer, 1994.
24. Mario Lamberger, Florian Mendel, Christian Rechberger, Vincent Rijmen, and Martin Schläffer. Rebound Distinguishers: Results on the Full Whirlpool Compression Function. In Matsui [25], pages 126–143.
25. Mitsuru Matsui, editor. *Advances in Cryptology - ASIACRYPT 2009, 15th International Conference on the Theory and Application of Cryptology and Information Security, Tokyo, Japan, December 6-10, 2009. Proceedings*, volume 5912 of *Lecture Notes in Computer Science*. Springer, 2009.
26. Krystian Matusiewicz, María Naya-Plasencia, Ivica Nikolic, Yu Sasaki, and Martin Schläffer. Rebound Attack on the Full Lane Compression Function. In Matsui [25], pages 106–125.
27. Florian Mendel, Thomas Peyrin, Christian Rechberger, and Martin Schläffer. Improved Cryptanalysis of the Reduced Grøstl Compression Function, ECHO Permutation and AES Block Cipher. In Jr. et al. [18], pages 16–35.
28. Florian Mendel, Christian Rechberger, Martin Schläffer, and Søren S. Thomsen. The Rebound Attack: Cryptanalysis of Reduced Whirlpool and Grøstl. In Dunkelman [13], pages 260–276.
29. Ralph C. Merkle. One Way Hash Functions and DES. In Brassard [8], pages 428–446.
30. Marine Minier, Raphael C.-W. Phan, and Benjamin Pousse. Distinguishers for Ciphers and Known Key Attack against Rijndael with Large Blocks. In Preneel [36], pages 60–76.
31. National Institute of Standards and Technology. FIPS 180-1: Secure Hash Standard. `http://csrc.nist.gov`, April 1995.
32. National Institute of Standards and Technology. FIPS PUB 197, Advanced Encryption Standard (AES). Federal Information Processing Standards Publication 197, U.S. Department of Commerce, November 2001.
33. National Institute of Standards and Technology. Announcing Request for Candidate Algorithm Nominations for a NewCryptographic Hash Algorithm (SHA-3) Family. *Federal Register*, 27(212):62212–62220, November 2007. Available:`http://csrc.nist.gov/groups/ST/hash/documents/FR_Notice_Nov07.pdf`(2008/10/17).
34. Phong Q. Nguyen, editor. *Progressin Cryptology - VIETCRYPT 2006, First International Conferenceon Cryptology in Vietnam, Hanoi, Vietnam, September 25-28, 2006, Revised Selected Papers*, volume 4341 of *Lecture Notes in Computer Science*. Springer, 2006.
35. Thomas Peyrin. Cryptanalysis of Grindahl. In Kaoru Kurosawa, editor, *ASIACRYPT*, volume 4833 of *Lecture Notes in Computer Science*, pages 551–567. Springer, 2007.
36. Bart Preneel, editor. *Progress in Cryptology - AFRICACRYPT 2009, Second International Conference on Cryptology in Africa, Gammarth, Tunisia, June 21-25, 2009. Proceedings*, volume 5580 of *Lecture Notes in Computer Science*. Springer, 2009.
37. RIPE. Integrity primitives for secure information systems. In A. Bosselaers and B. Preneel, editors, *Final Report of RACE Integrity Primitives Evaluation (RIPE-RACE 1040)*, volume 1007 of *Lecture Notes in Computer Science*. Springer, 1995.
38. Phillip Rogaway. Formalizing human ignorance. In Nguyen [34], pages 211–228.
39. Ronald L. Rivest. RFC 1321: The MD5 Message-Digest Algorithm. `http://www.ietf.org/rfc/rfc1321.txt`, April 1992.
40. Victor Shoup, editor. *Advances in Cryptology - CRYPTO 2005: 25th Annual International Cryptology Conference, Santa Barbara, California, USA, August 14-18, 2005, Proceedings*, volume 3621 of *Lecture Notes in Computer Science*. Springer, 2005.
41. David Wagner. A generalized birthday problem. In Yung [44], pages 288–303.
42. Xiaoyun Wang, Yiqun Lisa Yin, and Hongbo Yu. Finding collisions in the full sha-1. In Shoup [40], pages 17–36.
43. Xiaoyun Wang and Hongbo Yu. How to break md5 and other hash functions. In Cramer [9], pages 19–35.
44. Moti Yung, editor. *Advances in Cryptology - CRYPTO 2002, 22nd Annual International Cryptology Conference, Santa Barbara, California, USA, August 18-22, 2002, Proceedings*, volume 2442 of *Lecture Notes in Computer Science*. Springer, 2002.

Appendix A: the amount of freedom degrees

Once a differential path settled, a point has to be clarified: the amount of freedom degrees available to the attacker. Indeed, one has to evaluate how much valid pairs can be found for the whole differential trail. We want to ensure that enough solutions for the controlled rounds exist so that we have a good probability that at least one of them will fulfill the entire differential characteristic. Moreover, when

searching for semi-free-start collisions, we may even go further since we may require an important amount of valid candidates for the entire differential path.

Freedom degrees for ECHO

We use the same counting reasoning than in [16], except that we have to precisely evaluate what is the freedom degrees consumption for the various 2 AES-round differential transitions as well (in [16] it was implicitly assumed that all the BIG SubBytes transitions were $\mathtt{F} \rightarrow \mathtt{F}$, thus happening with probability very close to 1 and consuming no freedom degrees). For example, let us take the $\mathtt{D} \rightarrow \mathtt{1}$ transition through the BIG SubBytes in the forward direction: we require one AES MixColumns transition $4 \rightarrow 1$ which happens with probability 2^{-24}. Thus, if we have k valid candidates on the input, we obtain $k \times 2^{-24}$ valid candidates on the output of this layer and we consumed 2^{24} freedom degrees. The amount of freedom degrees consumed during a transition is the invert of the probability of success of this transition. Thus, with Table 2, it is very easy to compute the freedom degrees consumption for all the AES round transitions considered so far.

We illustrate the counting method by applying it to the example of the 7-round path from Figure 3. First, note that the start-from-the-middle attack will find **all** the possible internal states such that the controlled rounds are verified. We start from state $\mathsf{B.MC}_3^{in}$ (located between $\mathsf{B.ShR}_3$ and $\mathsf{B.MC}_3$). This state is fully active which means that we can start with $2^{2048 \times 2 - 1} = 2^{4095}$ distinct pairs. When going forward, the $\mathsf{B.MC}_3$ transition happens with probability $2^{-4 \times 24 \times 16} = 2^{-1536}$ and the transition through $\mathsf{B.MC}_4$ happens with probability $2^{-24 \times 16} = 2^{-384}$. All the other layers are verified with probability one so the forward computation consumes $2^{1536+384} = 2^{1920}$ freedom degrees. Then, during the backward computation, the sixteen $\mathtt{C} \leftarrow \mathtt{F} \leftarrow \mathtt{F}$ transitions through $\mathsf{B.SB}_3$ happen with probability $2^{-16 \times 96} = 2^{-1536}$ according to Table 2 ($\mathtt{C} \leftarrow \mathtt{F}$ with probability 2^{-96} and $\mathtt{F} \leftarrow \mathtt{F}$ with probability 1). Also, the four $\mathtt{D} \leftarrow \mathtt{1} \leftarrow \mathtt{C}$ transitions through $\mathsf{B.SB}_2$ happen with probability $2^{-4 \times 24} = 2^{-96}$ ($\mathtt{D} \leftarrow \mathtt{1}$ with probability 1 and $\mathtt{1} \leftarrow \mathtt{C}$ with probability 2^{-24}). Then, the BIG MixColumns transitions through $\mathsf{B.MC}_2$ are verified with probability $2^{-4 \times 4 \times 24} = 2^{-384}$ and through $\mathsf{B.MC}_1$ with probability $2^{-4 \times 24} = 2^{-96}$. All the other layers in the backward direction are verified with probability one. Overall, the backward computation consumes $2^{1536+384+96+96} = 2^{2112}$ freedom degrees. We can finally conclude that we started with 2^{4095} pairs from which only a factor $2^{-1920-2112} = 2^{-4032}$ will be valid for the whole differential path. One can then generate 2^{63} distinct valid pairs for the 7-round path from Figure 3.

Note that the differential paths we use are just instances among a family of good differential trails. For example, in the case of the 7-round path from Figure 3, instead of placing the active word on the top left position of $\mathsf{B.MC}_0^{out}$ (between $\mathsf{B.MC}_0$ and $\mathsf{B.SB}_1$), one could place it in the 15 others locations. Those new paths present the same properties than the original one and this reasoning also applies to the active word located in $\mathsf{B.MC}_4^{out}$ (between $\mathsf{B.MC}_4$ and $\mathsf{B.SB}_5$). As a consequence, the attacker manages $16^2 = 2^8$ different core paths which provides him 2^8 additional freedom degrees.

Finally, some additional freedom degrees can be obtained if one considers that the salt value can be fully controlled by the attacker. While this scenario is not very relevant in practice, it is interesting to see what the attacker is able to do in such a situation. In the case of ECHO, the salt value is 128-bit long and it then directly adds 2^{128} supplementary freedom degrees. To conclude, the attacker can generate 2^{71} distinct valid pairs for 7-round paths like the one depicted in Figure 3, and 2^{199} if he controls the salt. The same method is used for all the differential trails for ECHO considered in this article.

Freedom degrees for Grøstl

The case of Grøstl is easier to analyze since we don't have to handle word-wise and byte-wise truncated differentials at the same time. Yet, the same counting technique can be applied. Interestingly, for all the paths we provided concerning Grøstl, an attacker can expect only one solution for the whole trail with good probability. This explains why one can not really hope for a semi-free-start collision attack on reduced versions of Grøstl (such as 7 or 8-round versions) obtained with the paths given. Or, said in other words, a semi-free-start collision attack may be mounted, but will only work with a low probability.

As an example, we provide here the freedom degrees analysis for the 10-round differential path from Figure 15. By starting from the fully active internal state located at the output of MC_4, we begin with about $2^{512\times 2-1} = 2^{1023}$ distinct pairs of internal state values. When going forward, the first freedom degrees consuming operation is the MC_5 transition which happens with probability $2^{-7\times 56-48} = 2^{-440}$. Then, one byte is erased during AC_6 while the transition through MC_6 happens with probability 2^{-48} and in total this round consumes $2^{8+48} = 2^{56}$ freedom degrees. Finally, the last consuming operation when computing forward is AC_7 for which two bytes have to be erased (2^{16}). When computing backward, the MixColumns functions MC_3 and MC_2 requires $2^{48\times 8} = 2^{384}$ and $2^{2\times 56} = 2^{112}$ freedom degrees respectively. Then, two bytes are erased through AC_2 and all the other differential transitions consume nothing since they are deterministic. Finally, we started with 2^{1023} freedom degrees from which only a fraction $2^{440+8+48+16+384+112+16} = 2^{1024}$ will verify the whole differential path. Thus, since this reasoning is done on average, an attacker has a good probability to obtain one single solution for the whole differential path.

Appendix B: distinguishing the full internal permutation of ECHO-256

A 8-round core truncated differential path is given in Figure 5. Its usability is limited only to distinguish 8 rounds of the internal ECHO permutation (the full number of rounds for ECHO-256) and not a smaller number of rounds by cutting the beginning and/or the end of the trail. Indeed, the start-from-the-middle attack [27] can not be used anymore as too many active cells are present in the middle rounds. One has to use the Super-Sbox method instead, which is inefficient in the case of ECHO since it requires at least 2^{512} computations and memory.

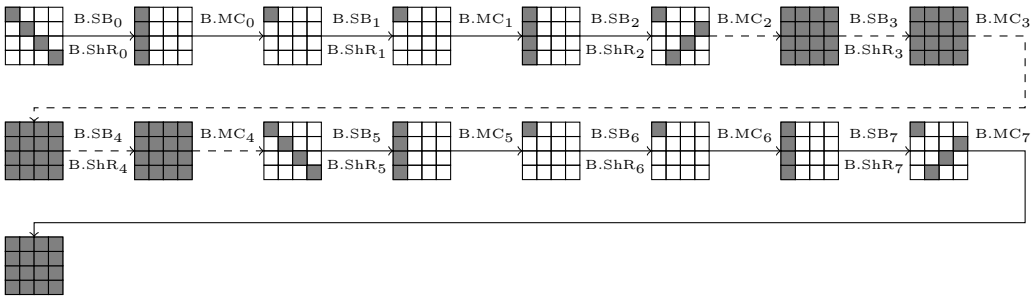

Fig. 5. Core truncated differential path for 8 rounds of the ECHO internal permutation. Each cell represents a 128-bit word and a gray cell stands for an active word. The controlled rounds are depicted with dashed lines.

From this core trail we derive the truncated differential path from Figure 6 for which one can obtain a valid candidate with a complexity of 2^{512} computations and memory. Indeed, the uncontrolled rounds are verified with probability 2^{-384} (because of the sixteen AES MixColumns transitions $4 \rightarrow 1$ through $\mathsf{B.MC}_5$), but the Super-Sbox forces a minimal cost of 2^{512}. Concerning the freedom degrees, the counting method from Appendix A shows that the attacker can generate a total of 2^{71} valid candidates for the whole differential path (and 2^{199} when the salt is controlled as well).

The solution pair has four active 128-bit words in the input and four active 128-bit words in the output (the last BIG MixColumns call is not taken in account since it is fully linear). The situation is exactly the same as for the 7-round distinguisher using path from Figure 3: by reusing the concept of *limited birthday distinguishers* [16] we deduce that for a random 2048-bit permutation, finding such a pair should require at least 2^{1024} operations.

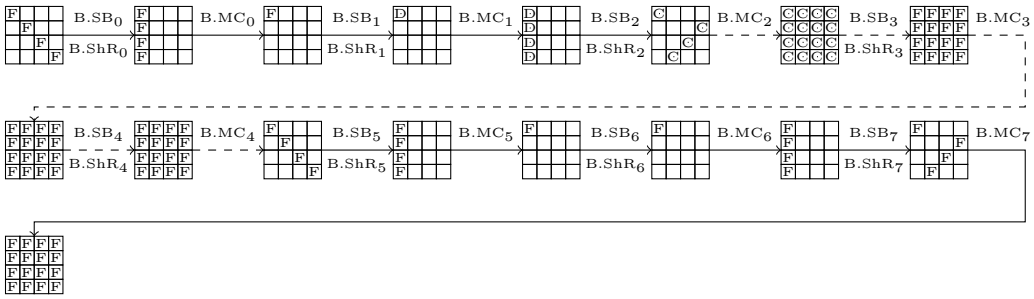

Fig. 6. 8-round differential path for the ECHO internal permutation. The controlled rounds are depicted with dashed lines.

The 8-round path from Figure 7 (also derived from the full core path from Figure 5) seems to be slightly better since the uncontrolled rounds are verified with probability $2^{-96-96} = 2^{-192}$ (because of the four $\mathtt{D} \leftarrow \mathtt{1} \leftarrow \mathtt{C}$ transitions through $\mathsf{B.SB}_5$ and the four AES MixColumns transitions $4 \rightarrow 1$ through $\mathsf{B.MC}_5$). However, the amount of freedom degrees is greatly reduced as the attacker has a very small probability 2^{-121} to actually find a single valid candidate for the whole differential path. Thus, this path is acceptable only if the salt can be controlled, which would lead to 2^7 distinct valid pairs for the whole differential trail.

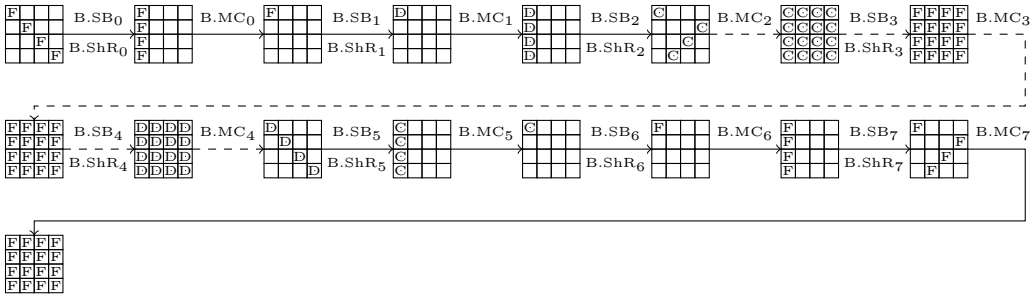

Fig. 7. 8-round differential path for the ECHO internal permutation. The controlled rounds are depicted with dashed lines.

The results concerning the internal permutation of ECHO are summarized in Table 3. Note that none of those distinguishers apply to the ECHO compression function due to the extra protection provided by the final shrinking stage of the compression function – namely its convolution effect on the output distribution of the permutation.

Table 3. Summary of results for the internal permutation of ECHO.

target	rounds	computational complexity	memory requirements	type	section
ECHO internal permutation	7	2^{384}	2^{64}	distinguisher	see [27]
	8	2^{768}	2^{512}	distinguisher	see [16]
	7	2^{96}	2^{64}	distinguisher	this paper
	8	2^{512}	2^{512}	distinguisher	this paper

Appendix C: the differential paths for the ECHO compression function

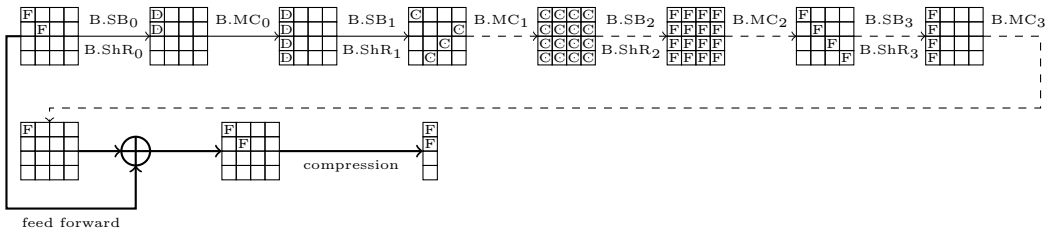

Fig. 8. 4-round differential path for the ECHO-256 compression function distinguisher. The controlled rounds are depicted with dashed lines.

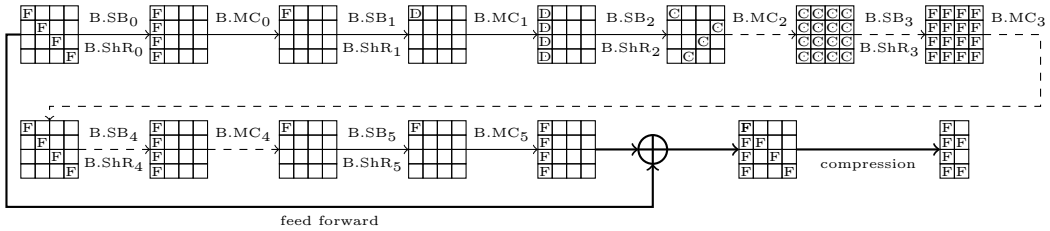

Fig. 9. 6-round differential path for the ECHO-512 compression function distinguisher. The controlled rounds are depicted with dashed lines.

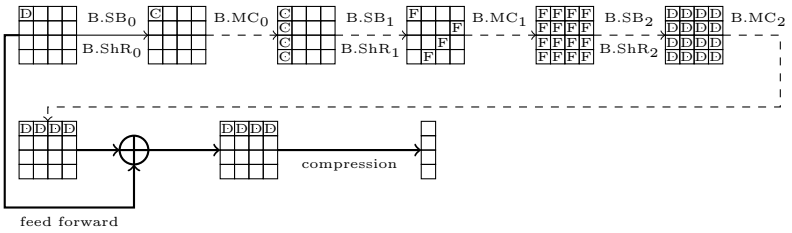

Fig. 10. 3-round differential path for the ECHO-256 compression function semi-free-start collision attack. The controlled rounds are depicted with dashed lines.

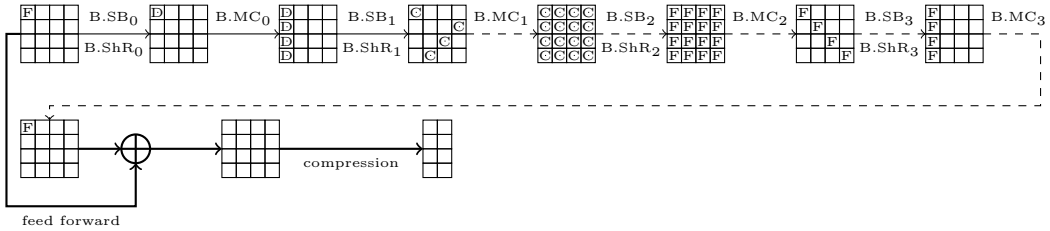

Fig. 11. 4-round differential path for the ECHO-512 compression function semi-free-start collision attack. The controlled rounds are depicted with dashed lines.

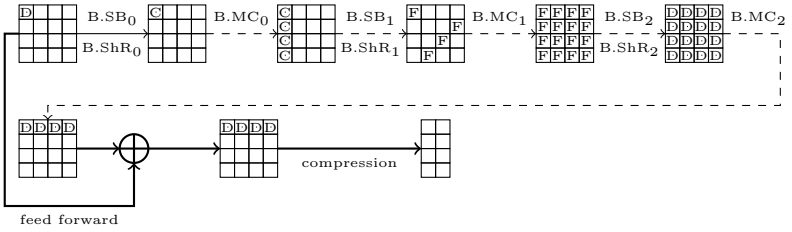

Fig. 12. 3-round differential path for the ECHO-512 compression function semi-free-start collision attack. The controlled rounds are depicted with dashed lines.

Appendix D: the ECHO-SP case

In the latest versions of the submission document [3], the authors propose a variant of ECHO, named ECHO-SP (for simple pipe). The specifications are exactly the same, but the final phase at the end of each compression function call outputs a n-bit chaining variable for a n-bit final hash value. Namely, the compression function of ECHO-SP-256 is identical to the one from ECHO-256 except that the two first words are xored with the two last words of the output column in order to obtain a 256-bit output chaining variable.

The compression function of ECHO-SP-512 is also identical to the one from ECHO-512 except that the first words column is xored with the second words column in order to obtain a 512-bit output chaining variable.

$$H' = \mathsf{comp}_{256sp}(P_E^8(H||M) \oplus H||M)$$

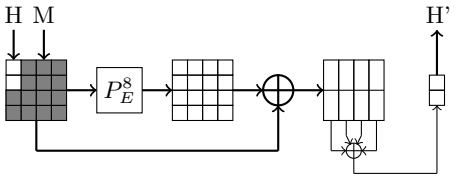

$$H' = \mathsf{comp}_{512sp}(P_E^{10}(H||M) \oplus H||M)$$

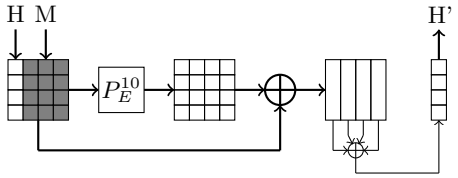

Since the number of rounds of the internal permutations remains the same for ECHO-SP, we only have to conduct again the analysis for deriving distinguishers or finding semi-free-start collisions for the compression function.

Concerning distinguishing attacks for the compression function, one can distinguish only 3 rounds for ECHO-SP-256. Namely, using the path from Figure 13, one can derive a distinguisher with complexity 2^{64} computations and memory. Actually, the uncontrolled rounds are verified with probability 1, thus the complexity comes from the minimal cost when using the start-from-the-middle technique to handle the controlled rounds. On the 256-bit output, we have only four bytes that may contain a difference and finding such a pair should require 2^{112} computations in the ideal case.

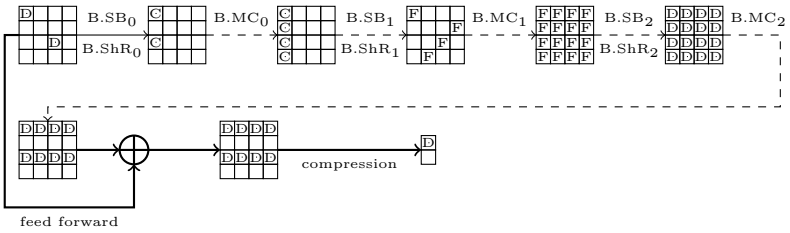

Fig. 13. 4-round differential path for the ECHO-SP-256 compression function distinguisher. The controlled rounds are depicted with dashed lines.

Since the compression function of ECHO-SP-512 is the same as the one from ECHO-256, we obtain exactly the same results. Namely, one can distinguish 4 rounds of the compression function with 2^{64} computations and memory.

Concerning the semi-free-start collision attacks for the compression function of ECHO-SP-256, the attack remains the same as for 3-round-reduced ECHO-256 (by using path from Figure 10). However, the 2^{224} computations and 2^{64} memory chosen-salt semi-free-start collision attack for 4 rounds is no more interesting since the generic birthday complexity is 2^{128} computations. Then, since the compression function of ECHO-SP-512 is the same as the one from ECHO-256, both attacks apply to 3 rounds and 4 rounds of ECHO-SP-512 respectively.

Finally, the results for ECHO-SP are summarized in Table 4.

Table 4. Summary of results for the ECHO-SP compression functions. ECHO-SP-256 and ECHO-SP-512 compression functions have 8 and 10 rounds respectively.

target	rounds	computational complexity	memory requirements	type	section
ECHO-SP-256	3	2^{64}	2^{64}	semi-free-start collision	this paper
comp. function	3	2^{64}	2^{64}	distinguisher	this paper
ECHO-SP-512	3	2^{64}	2^{64}	semi-free-start collision[1]	this paper
comp. function	4	2^{64}	2^{64}	distinguisher	this paper

Appendix E: the truncated differential paths for Grøstl

[1] A semi-free-start collision can be found for the 4-round reduced ECHO-SP-512 compression function with complexity 2^{224} computations and 2^{64} memory, if the salt value can be controlled by the attacker.

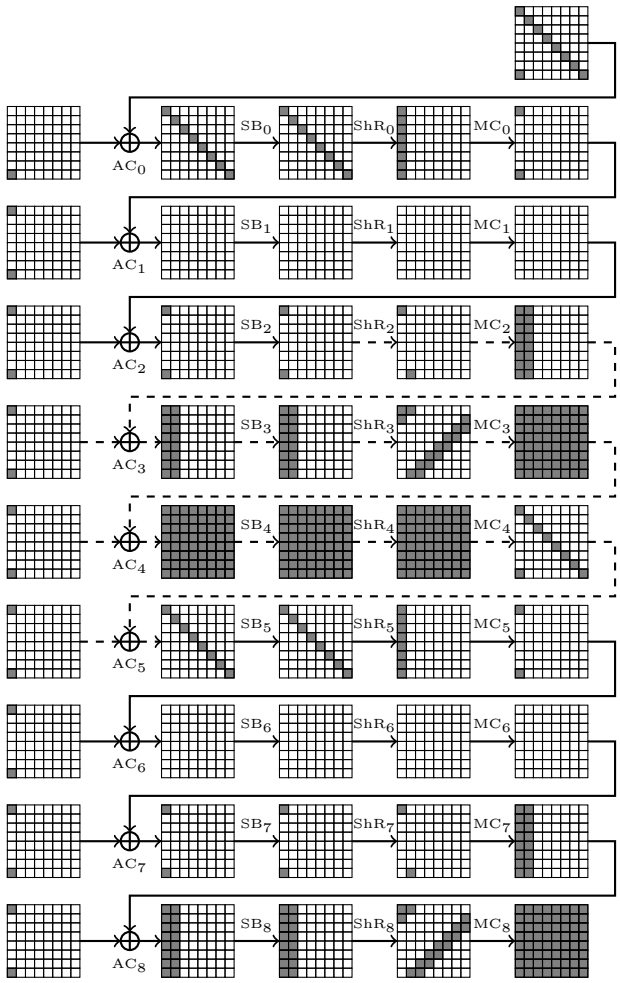

Fig. 14. 9-round differential path between P and Q for Grøstl-256. Each cell represents a byte and a gray cell stands for an active byte. The controlled rounds are depicted with dashed lines. The matrices on the left represent the differences incorporated during the AC layers.

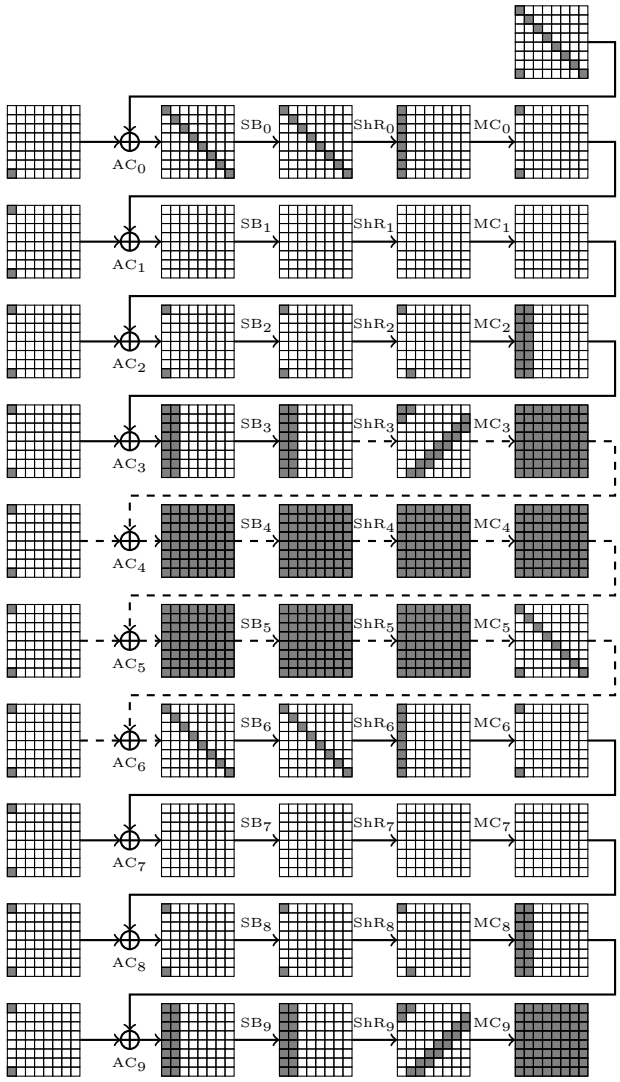

Fig. 15. 10-round differential path between P and Q for Grøstl-256. Each cell represents a byte and a gray cell stands for an active byte. The controlled rounds are depicted with dashed lines. The matrices on the left represent the differences incorporated during the AC layers.

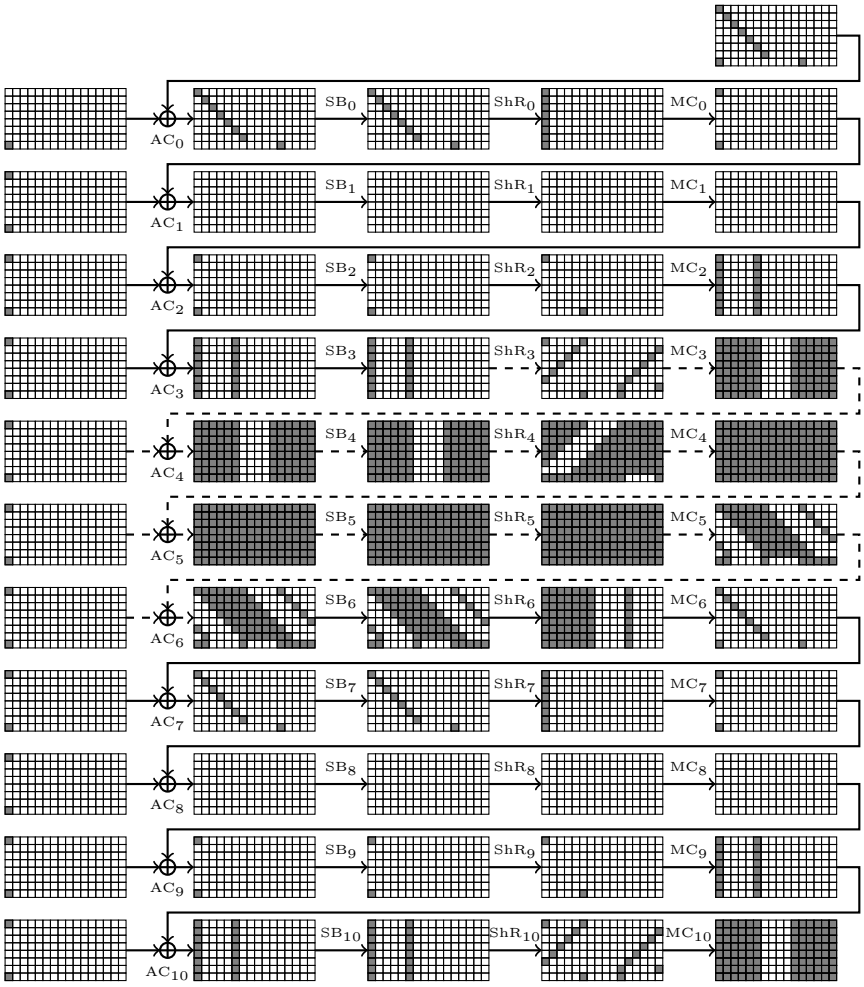

Fig. 16. 11-round differential path between P and Q for Grøstl-512. Each cell represents a byte and a gray cell stands for an active byte. The controlled rounds are depicted with dashed lines. The matrices on the left represent the differences incorporated during the AC layers.